ISBN: 978-3-95450-241-7 ISSN: 2673-5350 doi:10.18429/JACoW-IBIC2022-WEP24

MODELING AND EXPERIMENTAL EVALUATION OF A BUNCH ARRIVAL-TIME MONITOR WITH ROD-SHAPED PICKUPS AND A LOW-PI-VOLTAGE ULTRA-WIDEBAND TRAVELING WAVE ELECTRO-OPTIC MODULATOR FOR X-RAY FREE-ELECTRON LASERS*

A. Kuzmin†, E. Bründermann, C. Eschenbaum,C. Koos, A. Kotz, A.-S. Müller,
G. Niehues, A. Schwarzenberger, Karlsruhe Institute of Technology KIT, Karlsruhe, Germany
B. E. J. Scheible[1,‡], A. Penirschke, Technische Hochschule Mittelhessen, Friedberg, Germany
M. K. Czwalinna, H. Schlarb, Deutsches Elektronen-Synchrotron DESY, Hamburg, Germany
W. Ackermann, H. De Gersem, Technische Universität Darmstadt, Darmstadt, Germany
[1]also at Technische Universität Darmstadt, Darmstadt, Germany

Abstract

X-ray Free-Electron Laser (XFEL) facilities, such as the 3.4 km European XFEL, require long-range synchronization that necessitate the use all-optical links with electro-optic bunch arrival-time monitors (BAM). Current BAM systems achieve a resolution up to 3.5 fs for 250 pC bunches. Precise bunch arrival timing is essential for experiments, which study ultra-fast dynamical phenomena with highest temporal resolution. Future experiments will crucially rely on femtosecond pulses from bunch charges well below 20 pC. State-of-the-art BAMs are not allowing accurate timing for operation with such low bunch charges. Here, we report on the progress in the development of an advanced BAM based on rod-shaped pickups mounted on a printed circuit board and ultra-wideband travelling-wave electro-optic modulators with low operating voltages. We perform modeling and experimental evaluation for the fabricated pickups and electro-optic modulators and analytically estimate timing jitter for the advanced BAM system. Additionally, we discuss an experimental setup to demonstrate joint operation of new pickups and wideband EO modulators for low bunch charges less than 5 pC.

INTRODUCTION

X-ray Free-Electron Laser (XFEL) operation depends on a synchronization system with high timing stability and fs-precision [1]. Furthermore, precise bunch arrival timing between FEL and external laser pulses is essential for experiments, which study ultra-fast dynamical phenomena with highest temporal resolution [2]. For this reason, an all-optical synchronization system is implemented in several facilities, e.g. the 3.4 km long European XFEL [3].

This synchronization system is based on a pulsed optical reference, which is emitted by a commercial laser oscillator locked to the main oscillator for medium and long-term stability [1]. The reference laser pulses are distributed to different end-stations, e.g. electro-optic (EO) bunch arrival-time monitors (BAMs), via actively length-stabilized all-optical fiber links [1]. The BAM stations allow for precise arrival-time measurements by coupling to transient fields of every single bunch with cone-shaped pickups [1, 4, 5]. A bipolar radio-frequency (rf) pulse is fed to an electro-optic modulator (EOM) where the rf pulse is matched with the optical reference pulse [4]. The laser amplitude is modulated linearly to the arrival-time deviation, which can be determined afterwards in the data acquisition electronics [4].

The current BAMs achieve single bunch arrival-time measurements with a resolution of 3.5 fs for 250 pC bunches [6]. Experiments will crucially rely on fs pulses from bunch charges well below 20 pC. Therefore, an updated BAM for bunch charges lower than 5 pC is targeted. In this contribution the progress made in the two sub-projects is compiled and the overall improvement is estimated. Additionally, possibilities of the experimental demonstration are discussed.

NEW BAM DESIGN

In an ongoing project two components of the BAMs have been redesigned. The first objective was to update the pickups in order to increase the voltage signal by a factor of 10. The second objective was to develop and test a new electro-optical modulator which would allow further increase of timing resolution of a BAM. The new EOM has to be simultaneously broadband and has to feature low π-voltage.

Pickups

The state-of-the-art 40 GHz-pickups were shaped as a cone to reduce ringing and reflections by a constant line impedance [5]. In simulations they achieve 15 mV pC^{-1} ps^{-1} as normalized signal slew rate (SR), which is a decisive characteristic for the overall BAM sensitivity. The signal slope could be increased significantly by switching to an open-coax design with prolonged inner conductor, because of an increased active surface and reduced distance to the bunch [7]. Further improvement was found by implementation of these pickups in form of a rod mounted on a printed circuit board (PCB), their four signals are combined and fed to a common vacuum feedthrough [7]. This design surpassed the goal of 150 mV pC^{-1} ps^{-1} in simulations [7].

* Work supported by the German Federal Ministry of Education and Research (BMBF) under contract No. 05K19VKB and 05K19RO1.
† artem.kuzmin@kit.edu
‡ bernhard.scheible@iem.thm.de

ISBN: 978-3-95450-241-7 ISSN: 2673-5350 doi:10.18429/JACoW-IBIC2022-WEP24

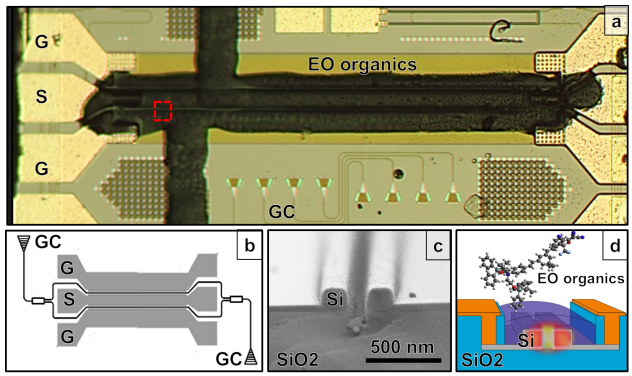

Figure 1: Silicon-Organic Hybrid MZM; **a:** optical image of 1-mm-long SOH-MZM with dispensed organic EO material; **b:** schematic representation of an MZM based on coplanar ground-signal-ground (GSG) electrodes, photonic waveguides and grating couplers (GC) for in/out -coupling of light; **c:** SEM image of a cross section of a Si slot-waveguide in one arm of MZM (region denoted with red square on **a**); **d:** schematic cross section of the SOH phase shifter.

EOMs

In the ongoing project we are developing Silicon-Organic Hybrid (SOH) traveling-wave Mach-Zehnder Modulators (MZM) with push-pull electrode configuration as shown in Fig. 1a. The schematic of an MZM with electrodes in ground-signal-ground (GSG) configuration forming a coplanar microwave waveguide is shown in Fig. 1b. The optical transmission, Tr, of an MZM with π-voltage, V_π, and optical insertion loss η_o, can be expressed as $\mathrm{Tr} = 1/2\eta_o\left[1+\cos\left(\phi+\pi V(t)/V_\pi\right)\right]$, where $V(t)$ is the signal voltage and ϕ is a dc optical phase shift between the arms, which defines the working point. The EO phase modulators in the two arms of the Mach-Zehnder interferometer are based on the integrated silicon slot-waveguides (see Fig. 1c, scanning electron microscope image of the waveguide cross section), formed by two parallel silicon rails with a typical width of 240 nm and height of 220 nm placed 140 nm apart. Such waveguides are fabricated by dry etching on the silicon-on-insulator platform (SOI). The optical mode is largely concentrated in the slot between rails. The slot is filled with an electro-optically active organic material, which is locally dispensed on the slot-waveguides (see Fig. 1d). The organic EO material is functionalized or "poled" in a vacuum chamber by heating the modulator chip up to the glass transition temperature of the EO material and applying a dc electric field between signal and ground in the same direction in both arms [8].

In the framework of this project, we considered two variations of SOH modulators that differ by the coupling approach of rf mode to the region with the optical mode. The *capacitively-coupled* (CC) SOH was in-house nano-fabricated and demonstrated an EO bandwidth of around 80 GHz, $V_\pi = 1.3$ V and the total optical loss, $\eta_o = 19$ dB [9], where 10 dB are attributed to the coupling loss through an on-chip grating couplers and can be eliminated using optical packaging with edge couplers, but due to fabrication complexity this is still an ongoing process. The *resistively-coupled* (RC) SOH employs highly-doped 70-nm-thin silicon slabs to connect electrodes with optical slot waveguide, which allows for lower π-voltages down to $V_\pi = 0.32$ V in 1-mm-long devices [8], but the bandwidth is limited by the RC-constant of slab-slot connection. The fabrication process of an RC-SOH is compatible with standard CMOS processes and was performed at an external foundry (Advanced Micro Foundaries, AMF, Singapore) in the framework of a multi-project wafer run based on our designs and modeling.

MODELING AND EXPERIMENTAL EVALUATION

The EO-Electrical (EO-E) response of the current generation of SOH was measured on the non-packaged RC-SOH chips using a 1550 nm cw-laser and the 110 GHz VectorStar Anritsu Vector Network Analyzer (VNA) with an ultra-fast Anritsu photodiode on a special probe-station developed in the ongoing project. The result is shown in Fig. 2 along with the modeled EO-E response based on optical and EM-simulations of a MZM in CST MWS and the analysis from Ref. [10]. The measured π-voltage is $V_\pi = 0.5$ V and the optical insertion loss is $\eta_o \approx 13$ dB.

The rms timing accuracy, σ_t, of a BAM system can be estimated using:

$$\sigma_t \approx \frac{\sigma_n}{\mathrm{SR}_{\mathrm{eff}}}, \tag{1}$$

where $\mathrm{SR}_{\mathrm{eff}}$ is the effective slew rate of the electrical pulse from the pickup structure modified by the response spectrum of the EOM, and σ_n is an equivalent input rms voltage noise of the modulator. This noise we model as a quadrature sum of independent noise sources added in the process of EO-E conversion and digitization of an incoming BAM pulse, $\sigma_n = \sqrt{\sigma_{\mathrm{RIN}}^2+\sigma_q^2+\sigma_{pd}^2+\sigma_{adc}^2+\ldots}$, where main contributions are from Relative Intensity Noise (RIN) of the laser, σ_{RIN}, optical quantum noise, σ_q, noise of a photodiode, σ_{pd}, characterized by its Noise Equivalent Power (NEP) and noise of an Analog-to-Digital Converter (ADC), σ_{adc}.

Here, we focus on the conventional direct detection scheme at the half-transmission point of MZM modulator and ignore noise from bunch charge fluctuations and pulsed laser jitter. To refer equivalent optical noises from the input of the photodiode to the input of the MZM, we use a small-signal transfer function of the MZM that can be derived from $\mathrm{Tr}(V)$-relation at the half-transmission point with $\phi = \pi/2$, with given π-voltage, V_π, and average input optical power P_o:

$$|\widetilde{H}_{\mathrm{mzm}}| = \frac{\partial \mathrm{Tr}}{\partial V} = \frac{\partial P_o/P_o}{\partial V} \approx \frac{\pi}{2\eta_o V_\pi}. \tag{2}$$

Additionally, we use the conversion gain of the photodiode, $|\widetilde{H}_{\mathrm{pd}}|$, to refer ADC noise to the MZM rf input. The contribution to the total equivalent rms voltage noise from rms optical power fluctuations σ_o: RIN, quantum noise and

ISBN: 978-3-95450-241-7 ISSN: 2673-5350 doi:10.18429/JACoW-IBIC2022-WEP24

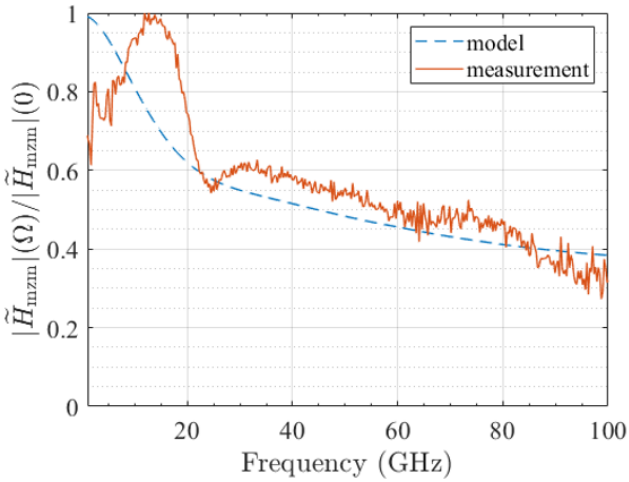

Figure 2: The normalized frequency dependence of the transfer function of RC-SOH MZM. The measured normalized transfer function at low frequency is lowered by the high output RF power provided by the VNA that caused over modulation.

NEP of the photodiode, denoted here as σ_{eoe}, then could be found as $\sigma_{\mathrm{eoe}} \approx |\widetilde{H}_{\mathrm{mzm}}|^{-1}(\sigma_{\mathrm{o}}/P_{\mathrm{o}})$:

$$\sigma_{\mathrm{eoe}} \approx \frac{2\eta_{\mathrm{o}} V_\pi}{\pi} \sqrt{\left(\frac{\delta P_{\mathrm{RIN}}}{P_{\mathrm{o}}}\right)^2 + \frac{2h\nu B}{P_{\mathrm{o}}} + \left(\frac{\mathrm{NEP}\sqrt{B}}{P_{\mathrm{o}}}\right)^2}, \quad (3)$$

where B is bandwidth of the ADC, δP_{RIN} is the rms RIN optical power fluctuations and $\nu \approx 193\,\mathrm{THz}$ is the optical frequency of the laser. The equivalent noise contribution from the ADC referred to the MZM rf input can be estimated using the known rms voltage noise, $\sigma_{v,\mathrm{adc}}$, of the ADC and the noise of a pre-amplifier, $\sigma_{v,\mathrm{amp}}$, with the gain G_{amp} :

$$\sigma_{\mathrm{adc}} \approx \frac{2\eta_{\mathrm{o}} V_\pi}{\pi P_{\mathrm{o}} |\widetilde{H}_{\mathrm{pd}}|} \sqrt{\sigma^2_{v,\mathrm{amp}} + \sigma^2_{v,\mathrm{adc}}/G_{\mathrm{amp}}}. \quad (4)$$

To calculate the effective slew rate, $\mathrm{SR}_{\mathrm{eff}}$ in Eq. (1), we use a simulated time trace of the BAM pulse ($\mathrm{SR}/q \approx 170\,\mathrm{mV\,pC^{-1}\,ps^{-1}}$ [7]) after attenuation in coaxial cables with normalized slew rate of $\mathrm{SR}/q \approx 130\,\mathrm{mV\,pC^{-1}\,ps^{-1}}$ and apply a filter that corresponds to the response spectrum of the EOM shown in Fig. 2. The resulting normalized slew rate, $\mathrm{SR}_{\mathrm{eff}}/q \approx 95\,\mathrm{mV\,pC^{-1}\,ps^{-1}}$, is about a factor of 1.5 smaller than the slew rate of the original pulse. For our jitter estimations we assume the average input laser power $P_{\mathrm{o}} \approx 5\,\mathrm{mW}$, relative intensity noise, $\delta P_{\mathrm{RIN}}/P_{\mathrm{o}} \approx 0.25\%$, the bandwidth of the ADC, $B = 200\,\mathrm{MHz}$ with typical SNR $\approx 70\,\mathrm{dBFS}$ and rms voltage noise $\sigma_{v,\mathrm{adc}} \approx 1\,\mathrm{mV}$ at 3 V full-scale, with a typical 200-MHz pre-amplifier rms-noise of $\sigma_{v,\mathrm{amp}} \approx 28\,\mu\mathrm{V}$, a gain of $G_{\mathrm{amp}} = 40\,\mathrm{dB}$, and a photodiode NEP $\approx 10\,\mathrm{pW}/\sqrt{\mathrm{Hz}}$ with conversion gain $|\widetilde{H}_{\mathrm{pd}}| \approx 400\,\mathrm{V\,W^{-1}}$. With the above specified parameters, π-voltage of the modulator, $V_\pi \approx 0.5\,\mathrm{V}$ and insertion loss $\eta_{\mathrm{o}} = 13\,\mathrm{dB}$ the estimated rms timing jitter (from Eq. (1)) amounts to $\sigma_t \approx 9\,\mathrm{fs}$ for a bunch charge of 1 pC. The contribution from RIN is about an order of magnitude larger than the contribution from quantum and photodiode noises, which are comparable. The contribution from the electronic noise of the back-end is insignificant.

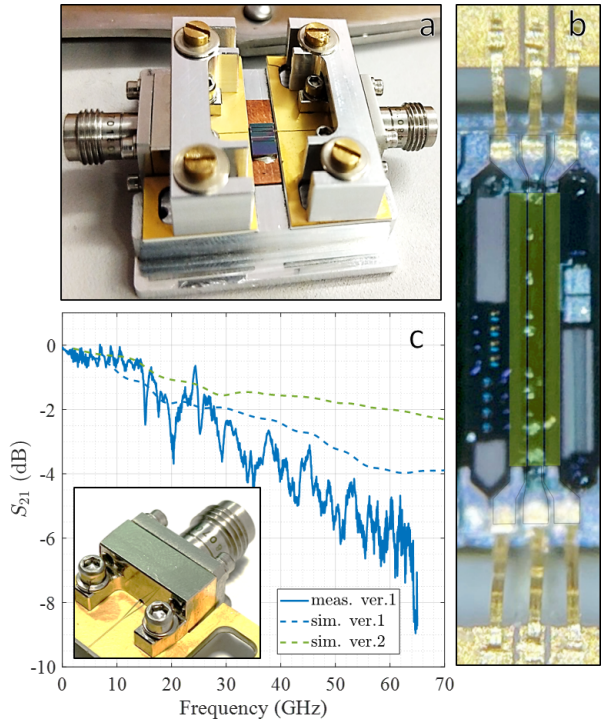

Figure 3: The prototype of the packaging solution for the SOH modulator; **a** the package with mounted rf-adapter PCBs from both sides of the chip. The openings from the sides are for the mounting the v-groove fiber arrays; **b** The optical microscope image of the SOH MZM connected to rf-adapter PCBs using golden ribbon bonds; **c** the measured and simulated rf transmission of the connectorized PCB; the green dashed curve demonstrates simulation of the second version of PCB with improved performance.

OUTLOOK

For the joint demonstration of a new BAM prototype, which employs the new pickups [7] and the EOMs presented here, we are developing microwave and optical packaging solution for SOH chips. The first version of the package is presented in Fig. 3a. The package is based on 1.85 mm-connectors ("V") and gold-plated alumina rf-adapter boards (inset in Fig. 3b). The rf-adapter boards are designed in a form of a tapered coplanar waveguide and laser-etched with a signal line width of 80 µm and a gap width of 25 µm. The chip is connected to the rf-adapter board using golden ribbon bonds (Fig. 3c). The graph in Fig. 3b shows the rf transmission measurements and EM-simulation of the first version of the assembly are shown in the inset. The simulation of the second version of the assembly is shown by the green dashed line. It features an improved transmission

ISBN: 978-3-95450-241-7 ISSN: 2673-5350 doi:10.18429/JACoW-IBIC2022-WEP24

and will be tested in the future. For the optical coupling, the v-groove optical fiber array will be aligned and glued to the edge couplers on the chip. The joint testing with non-hermetic pickup rod-shaped prototypes and a packaged SOH-EOM are planned at the test facility FLUTE at KIT with fs-short bunch charges as low as a few pC. The balanced photo-detection scheme with dual-output MZM will be tested to suppress a contribution from relative intensity noise [11, 12].

CONCLUSION

The new EOM prototypes for BAM were successfully fabricated and tested. The timing jitter of a BAM system is estimated based on the obtained slew rates from the new rod-shaped pickups and measured EO conversion efficiency and bandwidth of new silicon-organic hybrid (SOH) modulators. A jitter-charge product of $\sigma_t \times q \approx 9\,\mathrm{fs\,pC}$ is calculated for the normalized signal slew rate of $150\,\mathrm{mV\,pC^{-1}\,ps^{-1}}$ of the new pickups, a π-voltage of the EOM of $V_\pi = 0.5\,\mathrm{V}$ and its measured frequency response. The estimated timing resolution of a BAM is strongly dominated by the relative intensity noise, $\sigma_P/P \approx 0.25\%$, of the pulsed laser, which is about an order of magnitude larger than the contributions from quantum and photodiode noises. Using a balanced photo-detection scheme, and employing a dual-output SOH modulator with 180° phase difference between its outputs will enable at least 20 dB suppression of RIN noise. In this case the timing jitter of the BAM will be fundamentally limited only by the optical quantum noise and the available laser power.

REFERENCES

[1] S. Schulz *et al.*, "Femtosecond all-optical synchronization of an X-ray free-electron laser", *Nat. Commun.*, vol. 6, p. 5938, 2015. doi:/10.1038/ncomms6938

[2] E. J. Jaeschke, S. Khan, J. R. Schneider, and J. B. Hastings, *Synchrotron light sources and free-electron lasers: Accelerator physics, instrumentation and science applications*, 2nd Edition, Cham: Springer International Publishing, 2020. doi:10.1007/978-3-030-23201-6

[3] T. Lamb *et al.*, "Large-scale optical synchronization system of the European XFEL with femtosecond precision", in *Proc. IPAC'19*, Melbourne, Australia, May 2019, pp. 3835–3838. doi:10.18429/JACoW-IPAC2019-THPRB018

[4] F. Löhl *et al.*, "Electron bunch timing with femtosecond precision in a superconducting free-electron laser", *Phys. Rev. Lett.*, vol. 104, no. 14, p. 144801, Apr. 2010. doi:10.1103/PhysRevLett.104.144801

[5] A. Angelovski *et al.*, "Pickup signal improvement for high bandwidth BAMs for FLASH and European - XFEL", in *Proc. IBIC'13*, Oxford, UK, Sep. 2013, paper WEPC40, pp. 778–781.

[6] M. K. Czwalinna *et al.*, "Beam arrival stability at the European XFEL", in *Proc. IPAC'21*, Campinas, Brazil, May 2021, pp. 3714–3719. doi:10.18429/JACoW-IPAC2021-THXB02

[7] B. E. J. Scheible *et al.*, "Bunch arrival-time measurement with rod-shaped pickups on a printed circuit board for X-ray free-electron lasers", in *Proc. IBIC'21*, Pohang, Korea, Sep. 2021, pp. 417. doi:10.18429/JACoW-IBIC2021-WEPP19

[8] C. Kieninger *et al.*, "Ultra-high electro-optic activity demonstrated in a silicon-organic hybrid modulator", *Optica*, vol. 5, no. 6, p. 739, Jun. 2018. doi:10.1364/OPTICA.5.000739

[9] S. Ummethala *et al.*, "Hybrid electro-optic modulator combining silicon photonic slot waveguides with high-k radio-frequency slotlines", *Optica*, vol. 8, no. 4, p. 511, Apr. 2021. doi:10.1364/optica.411161

[10] H. Zwickel *et al.*, "Verified equivalent-circuit model for slot-waveguide modulators", *Opt. Express*, vol. 28, no. 9, p. 12951, Apr. 2020. doi:10.1364/oe.383120

[11] K. Kikuchi, "Fundamentals of coherent optical fiber communications", *J. Lightwave Technol.*, vol. 34, no. 1, p. 157–179, Jan. 2016. doi:10.1109/jlt.2015.2463719

[12] M. Endo, T. D. Shoji, and T. R. Schibli, "High-sensitivity optical to microwave comparison with dual-output Mach-Zehnder modulators", *Sci. Rep.*, vol. 8, no. 1, Mar. 2018. doi:10.1038/s41598-018-22621-1